Journal of Solid State Chemistry **162,** 322–326 (2001)
doi:10.1006/jssc.2001.9327, available online at http://www.idealibrary.com on IDEAL®

New Members of the $(Ba_8Co_6O_{18})_\alpha(Ba_8Co_8O_{24})_\beta$ Polysomatic Series

J. M. González-Calbet,[1] K. Boulahya, M. L. Ruiz, and M. Parras

Departamento de Química Inorgánica, Facultad de Químicas, Universidad Complutense, 28040-Madrid, Spain

IN HONOR OF PROFESSOR PAUL HAGENMULLER ON THE OCCASION OF HIS 80TH BIRTHDAY.

The accurate control of both stoichiometry and synthesis conditions has allowed the stabilization of new Ba–Co oxides with one-dimensional structures related to the 2H-ABO_3 hexagonal perovskite. $Ba_{26}Co_{23}O_{69}$, $Ba_{44}Co_{39}O_{117}$, and $Ba_{28}Co_{25}O_{75}$ are new members of the $(Ba_8Co_6O_{18})_\alpha(Ba_8Co_8O_{24})_\beta$ polysomatic orthorhombic series whose structural features have been characterized by electron diffraction and high-resolution electron microscopy. These polysomes are described as the ordered intergrowth between structural slabs of one-half unit cell of the o-$Ba_8Co_7O_{21}$ and one $Ba_8Co_8O_{24}$ 2H-block in different ratios. © 2001 Elsevier Science

Key Words: **2H-related perovskite; electron diffraction; high-resolution electron microscopy; $(Ba_8Co_6O_{18})_\alpha(Ba_8Co_8O_{24})_\beta$ polysomes; $Ba_{26}Co_{23}O_{69}$; $Ba_{28}Co_{25}O_{75}$; $Ba_{44}Co_{39}O_{117}$.**

INTRODUCTION

The concept of polysomatism is used to define structures that can be created by combining two or more structurally and stoichiometrically distinct types of slab modules (1). Polysomatic series are groups of solids whose structures are made up of different ratios of the same types of slabs. Significant examples of polysomes were initially reported by Hagenmuller and his group in the course of their research in compositional variations in perovskite-related materials. Actually, they discovered the homologous series $A_nB_nO_{3n-1}$ (2, 3), composed of a series of polysomes formed by the intergrowth of the basic structural motifs of ABO_3 perovskite (4) and $A_2B_2O_5$ brownmillerite (5) type structures.

Polysomatic series have also been reported for one-dimensional oxides related to the 2H-hexagonal perovskite type. The stacking of A_3O_9 and A_3BO_9 layers leads to a series of polysomes (6–8) formed by the ordered intergrowth between the 2H-$BaNiO_3$ (9) and Sr_4PtO_6 (10) structural fragments. On the basis of this behavior and after the careful selection of A cation, a high number of oxides have been stabilized, keeping $B = Co$ constant, in the rhombohedral polysomatic series $(A_3Co_2O_6)_\alpha(A_3Co_3O_9)_\beta$ (A = Ca, Sr, Ba) (11–13). All of them are formed by the ordered intergrowth of the two smallest structural units in the above formula. In polyhedral terms their structures can be described as isolated infinite CoO_3 chains, running parallel to the c-axis, consisting of alternating octahedra and trigonal prismatic polyhedra sharing faces separated by A cations.

In recent papers, we have shown that the careful control of the synthesis conditions of Ba–Co mixed oxides leads to a different homologous series with the composition $(Ba_8Co_6O_{18})_\alpha(Ba_8Co_8O_{24})_\beta$ (14, 15). All the polysomes constituting this series exhibit orthorhombic symmetry and some of them are polytypes of the corresponding rhombohedral oxides, keeping in every row the same polyhedra sequence but a different spatial arrangement between such rows. α and β denote the number of each block constituting every phase, both corresponding to a hexagonal stacking sequence of layers, which in the former is constituted by alternating of $Ba_8Co_2O_{18}$ and Ba_8O_{24} layers whereas the latter shows only Ba_8O_{24} layers. Actually, from a hexagonal AO_3 layer with a_{2H} and b_{2H} parameters, the substitution of three oxygen atoms by one B cation following the $[10\bar{1}0]_{2H}$ and equivalent directions leads to a layer with the composition $A_8B_2O_{18}$ showing orthorhomic symmetry and parameters $a_0 = 2a_{2H}$; $b_0 = 2\sqrt{3}a_{2H}$ (Fig. 1). The oxides previously reported in this series are gathered in Table 1 and their structural models depicted in Fig. 2. The first member, o-$Ba_8Co_7O_{21}$, is formed by the alternation of one Ba_8O_{24} layer and one $Ba_8Co_2O_{18}$ layer. Members with an even number of Ba atoms per unit formula show a constant number of octahedra separating the trigonal prisms, but those with an odd number of Ba atoms are formed by the ordered intergrowth between the upper and lower adjacent terms.

Alternatively, their structures can be regarded as the ordered intergrowth between structural slabs of one-half unit cell of the o-$Ba_8Co_7O_{21}$ phase (o refers to orthorhombic symmetry) and one $Ba_8Co_8O_{24}$ 2H-block and can be considered as polysomatic structures. According to Veblen

[1]To whom correspondence should be addressed. Fax: 34 91 394 4352. E-mail: jgcalbet@quim.ucm.es.

0022-4596/01 $35.00

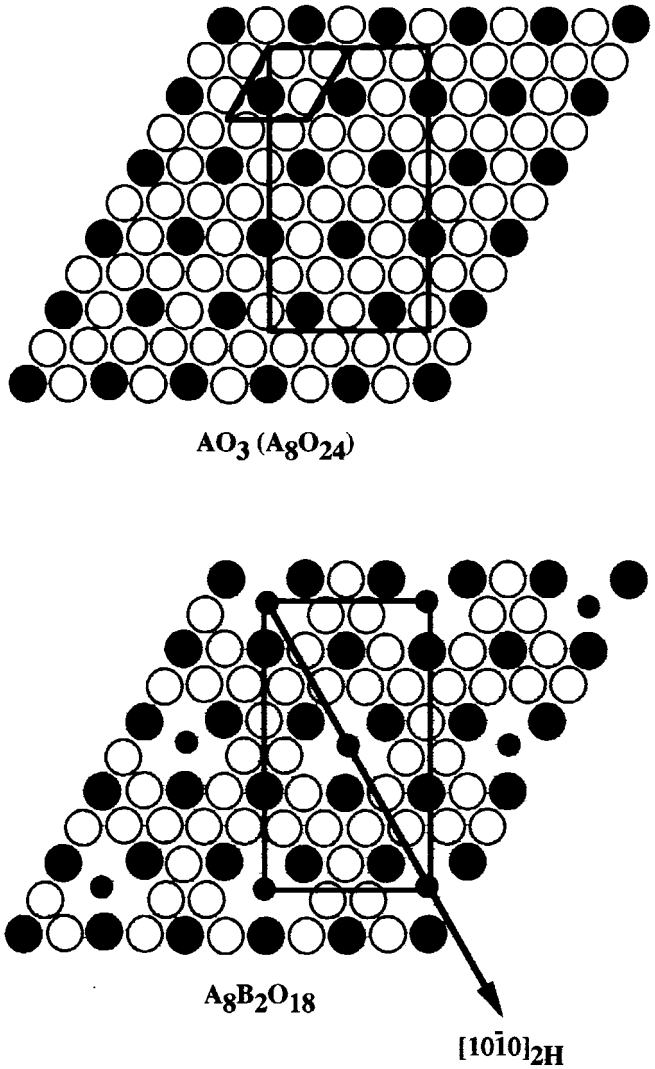

FIG. 1. Schematic representation of AO_3 (or A_8O_{24} per orthorhombic unit) and orthorhombic $A_8B_2O_{18}$ layers.

(16) a requirement for forming a polysome is that the energy of the interfaces between the component slabs must not be too large. This implies that the components must possess quasi-planar surfaces with very similar structures and lattice translations that are nearly equal to integral mutiples of each other. The mating surfaces of polysomatic slabs with the same symmetry facilitate the formation of new polysomes, as shown, for instance in the biopyribole series (17). *o*-$Ba_9Co_8O_{24}$ having ordered intergrowth between *o*-$Ba_8Co_7O_{21}$ and *o*-$Ba_{10}Co_9O_{27}$ (hereinafter referred as *o*-8 : 7 and *o*-10 : 9, respectively), the stabilization of new polysomes containing two or more of these repeating units cannot be discarded.

We report in this paper the structural characterization by means of selected area electron diffraction (SAED) and high-resolution electron microscopy (HREM) of new orthorhombic materials with the composition $Ba_{26}Co_{23}O_{69}$, $Ba_{44}Co_{39}O_{117}$, and $Ba_{28}Co_{25}O_{75}$ as a result of different intergrowth paths between *o*-8 : 7 and *o*-10 : 9 slabs.

TABLE 1

Chemical Composition, Number of Blocks (α and β), and Polyhedral Sequence per Row of the Phases Reported Up to Now Belonging to the $(Ba_8Co_6O_{18})_\alpha(Ba_8Co_8O_{24})_\beta$ Series

Composition	α	β	Stacking sequence[a]
$Ba_8Co_7O_{21}$	1	1	[1TP : $6O_h$]
$Ba_9Co_8O_{24}$	4	5	[1TP : $6O_h$][1TP : $8O_h$]
$Ba_{10}Co_9O_{27}$	2	3	[1TP : $8O_h$]
$Ba_{11}Co_{10}O_{30}$	4	7	[1TP : $8O_h$][1TP : $10O_h$]
$Ba_{12}Co_{11}O_{33}$	1	2	[1TP : $10O_h$]

[a] O_h = octahedron; TP = trigonal prism.

EXPERIMENTAL

$Ba_{26}Co_{23}O_{69}$, $Ba_{44}Co_{39}O_{117}$, and $Ba_{28}Co_{25}O_{75}$ were prepared by heating in air stoichiometric amounts of

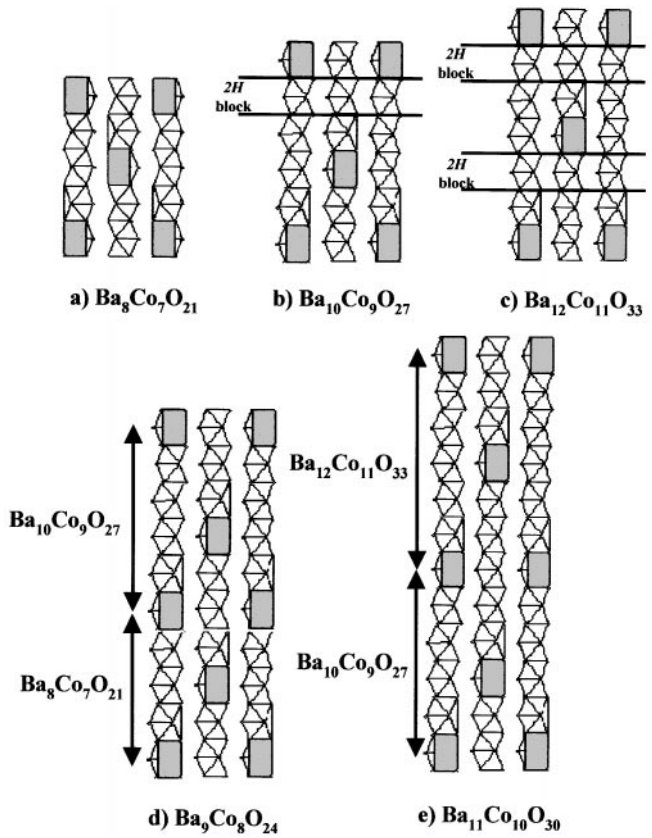

FIG. 2. Schematic representation of the structural models corresponding to the different members belonging to the $(Ba_8Co_6O_{18})_\alpha(Ba_8Co_8O_{24})_\beta$ series.

$BaCO_3$ and Co_3O_4 at 875°C for 3, 4, and 5 days, respectively. The average cationic composition was determined by inductive coupling plasma. The local composition in every crystal was established by energy dispersive spectroscopy (EDS) on a JEOL 2000FX electron microscope equipped with an energy-dispersive system LINK AN10000. Results are consistent with the nominal compositions. It is worth mentioning that the close Co/Ba ratio exhibited by these oxides makes difficult the differentation between them. However, electron diffraction patterns and high-resolution images allow an unambiguous characterization of each phase. The oxygen content was determined within $\pm 10^{-2}$ from the average oxidation state of cobalt analized by titration using Mohr's salt.

Powder X-ray diffraction (XRD) was carried out on a Philips X'Pert diffractometer using Cu$K\alpha$ radiation. SAED was performed on a JEOL 2000FX electron microscope, fitted with a double-tilting goniometer stage ($\pm 45°$). In order to be sure about the homogeneity of the samples, more than 50 crystals were checked in each case. HREM was performed on a JEOL 4000EX electron microscope, fitted with a double-tilting goniometer stage ($\pm 25°$), working at 400 kV. Samples were ultrasonically dispersed in *n*-butanol and transferred to carbon-coated copper grids.

RESULTS AND DISCUSSION

The XRD patterns corresponding to $Ba_{26}Co_{23}O_{69}$, $Ba_{44}Co_{39}O_{117}$, and $Ba_{28}Co_{25}O_{75}$ show characteristics similar to those shown in Fig. 1 of Ref. (15). Due to the striking similarity between the different oxides constituting this series, a SAED and HREM study has been performed, in order to elucidate the structure of these new phases.

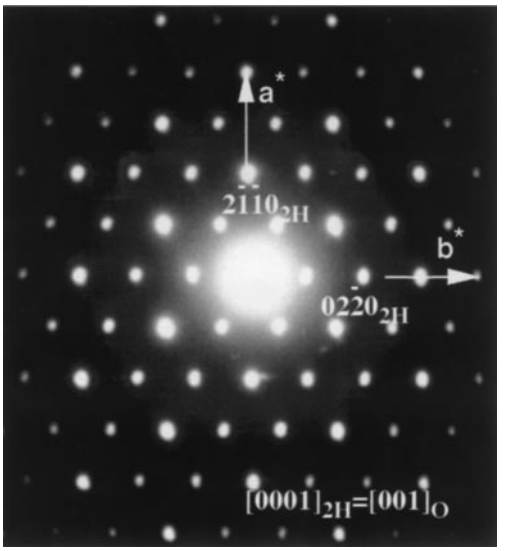

FIG. 3. SAED pattern of $Ba_{26}Co_{23}O_{69}$ along $[0001]_{2H}$. Identical patterns are obtained for $Ba_{28}Co_{25}O_{75}$ and $Ba_{44}Co_{39}O_{117}$ along this projection.

SAED clearly shows that all materials present orthorhombic symmetry and the same features as those previously reported (14, 15). In fact, the unit cell bases are identical since all of them show the same (*ab*)* reciprocal plane, as seen in Fig. 3, confirming that $a_0 = 2a_{2H}$; $b_0 = 2\sqrt{3}a_{2H}$ in all cases. We will show in the following the data corresponding to the main projection $[1\bar{2}10]_{2H}$.

Figure 4 shows the SAED pattern (a) and the HREM image (b) along $[1\bar{2}10]_{2H}$ corresponding to $Ba_{26}Co_{23}O_{69}$. The most intense reflections correspond to $(10\bar{1}0)_{2H}$ and $(0001)_{2H}$ and equivalent planes (subindex 2H refers to the

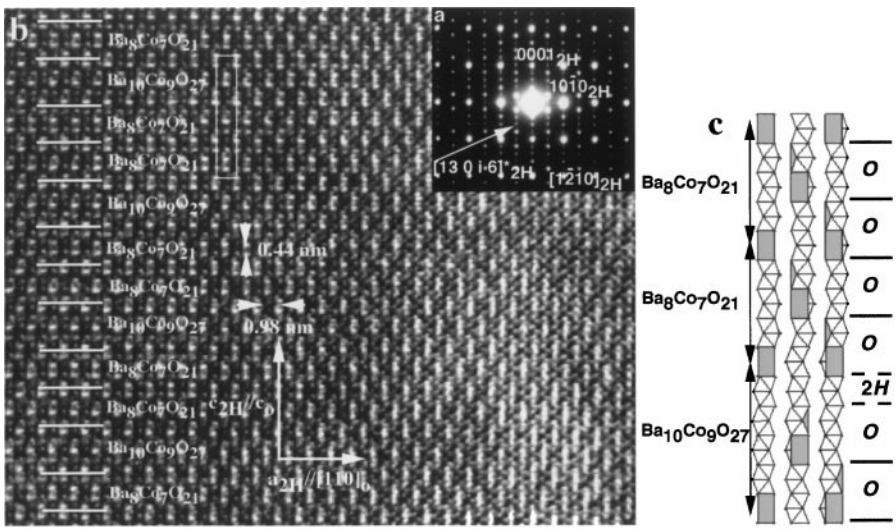

FIG. 4. (a) SAED and (b) HREM of $Ba_{26}Co_{23}O_{69}$ along $[1\bar{2}10]_{2H}$. (c) $Ba_{26}Co_{23}O_{69}$ structural model.

2H-$BaNiO_3$ structural type). A 26-fold modulated superstructure along $[13\ 0\ i\ 6]^*_{2H}$ and equivalent directions is apparent. Both XRD and SAED patterns can be indexed according to an orthorhombic unit cell with parameters $a = 1.14$ nm, $b = 1.98$ nm, and $c = 5.72$ nm. All reflections appearing in the SAED patterns can be indexed on the basis of conventional three-dimensional lattices, thus confirming that the structure is commensurate. They can be described from the 2H basic unit cell with the modulation given by a vector $\mathbf{k}$, perpendicular to the planes $(\alpha + \beta\ 0\ i\ \alpha)^*_{2H}$, which can be expressed as $\mathbf{k} = (1/2)a^*_{2H} + m2c^*_{2H}$, $m = \alpha/4(\alpha + \beta)$. From this, the $\alpha = 6$, $\beta = 7$ values can be obtained and the modulation vector for $Ba_{26}Co_{23}O_{69}$ is $\mathbf{k} = 1/2(a^*_{2H}) + 3/26(2c^*_{2H})$. The corresponding HREM image shows an ordered intergrowth between two unit cells of $Ba_8Co_7O_{21}$ and one $Ba_{10}Co_9O_{27}$ unit cell, in agreement with the nominal composition. Twenty-six layers, 12 $Ba_8Co_2O_{18}$ and 14 Ba_8O_{24}, constitute the unit cell corresponding to the $Ba_{26}Co_{23}O_{69}$ phase, leading to a $[1TP:6O_h][1TP:6O_h][1TP:8O_h]$ polyhedra sequence in every row (Fig. 4c). Therefore, this phase is a new member of the homologous series $(Ba_8Co_6O_{18})_\alpha(Ba_8Co_8O_{24})_\beta$, with a variable number of octahedra between trigonal prisms per row.

Since o-8:7 and o-10:9 are able to intergrow with a stacking sequence 1:1 [see Ref. (15)] but also following the 2:1 path, as shown above, the nominal composition $Ba_{28}Co_{25}O_{75}$ was prepared in order to check if other possibilities, such as the 1:2 ordering, also existed. Once again, SAED and HREM are adequate tools to elucidate the real intergrowth between the slabs constituting this new polysome. Figure 5 shows the SAED pattern (a) and the HREM image (b) along $[1\bar{2}10]_{2H}$ corresponding to $Ba_{28}Co_{25}O_{75}$. A 14-fold modulated superstructure can be observed following the $[7\ 0\ i\ 3]^*_{2H}$ direction. Such a superlattice is defined by a modulation vector $\mathbf{k} = 1/2(a^*_{2H}) + 3/28(2c^*_{2H})$. According to that, $\alpha = 3$, $\beta = 4$, i.e., $3(Ba_8Co_6O_{18})$ blocks and $4(Ba_8Co_8O_{24})$ blocks intergrow, per unit cell, along the c-axis. This is in agreement with the contrast observed in the structure image (Fig. 5b) where an apparently well ordered material is seen, whose structure can be described as an ordered intergrowth between one unit cell of $Ba_8Co_7O_{21}$ and two unit cells of $Ba_{10}Co_9O_{27}$ according to the sequence 1:2. Twenty-eight layers, 12 $Ba_8Co_2O_{18}$ and 16 Ba_8O_{24}, constitute the unit cell of the $Ba_{28}Co_{25}O_{75}$ phase, leading to a $[1TP:6O_h][1TP:8O_h][1TP:8O_h]$ polyhedra sequence in every row (Fig. 5c). Unit cell parameters corresponding to $Ba_{28}Co_{25}O_{75}$ are $a = 1.14$ nm, $b = 1.98$ nm, and $c = 6.16$ nm.

It is worth mentioning that in order to stabilize these phases, besides an adequate control of the stoichiometry, an accurate control of both temperature and annealing time is required. Since the annealing time increases as the Co/Ba ratio decreases, we have prepared an intermediate composition to check if a new ordering scheme arises between o-8:7 and o-10:9 phases. $Ba_{44}Co_{39}O_{117}$ is the nominal composition corresponding to three unit cells of $Ba_8Co_7O_{21}$ plus two unit cells of $Ba_{10}Co_9O_{27}$. SAED and HREM reveals the ordering of the slabs constituting this new polysome. Figure 6 shows the SAED pattern (a) and the HREM image (b) along $[1\bar{2}10]_{2H}$ corresponding to $Ba_{44}Co_{39}O_{117}$. The structural features are similar to those previously shown. Now, the modulation direction, perpendicular to the planes containing Co atoms in trigonal prisms, is $[11\ 0\ i\ 5]^*_{2H}$, intermediate between $[13\ 0\ i\ 6]^*_{2H}$ and $[7\ 0\ i\ 3]^*_{2H}$. A 22-fold modulated superstructure along such a direction is seen. This pattern is in agreement with an orthorhombic unit cell with parameters $a = 1.14$ nm, $b = 1.98$ nm, and $c = 9.68$ nm, the modulation vector being $\mathbf{k} = 1/2(a^*_{2H}) +$

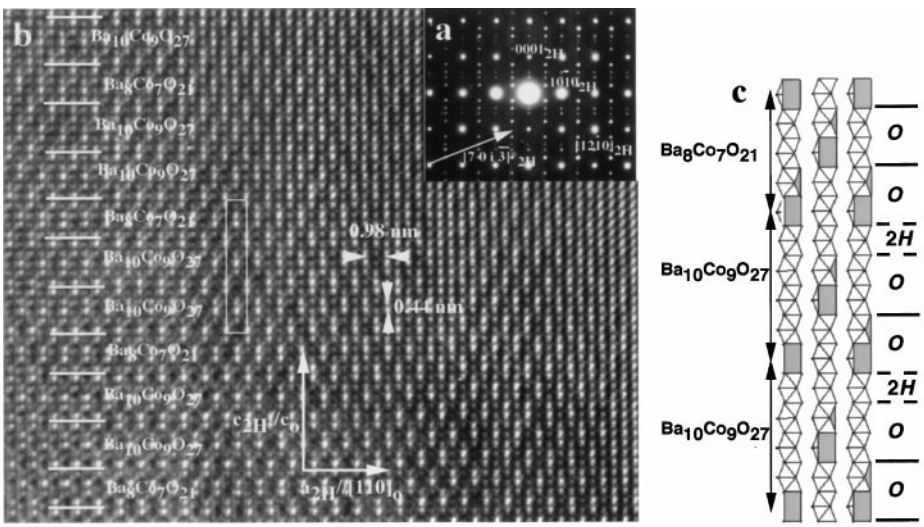

FIG. 5. (a) SAED and (b) HREM of $Ba_{28}Co_{25}O_{75}$ along $[1\bar{2}10]_{2H}$. (c) $Ba_{28}Co_{25}O_{75}$ structural model.

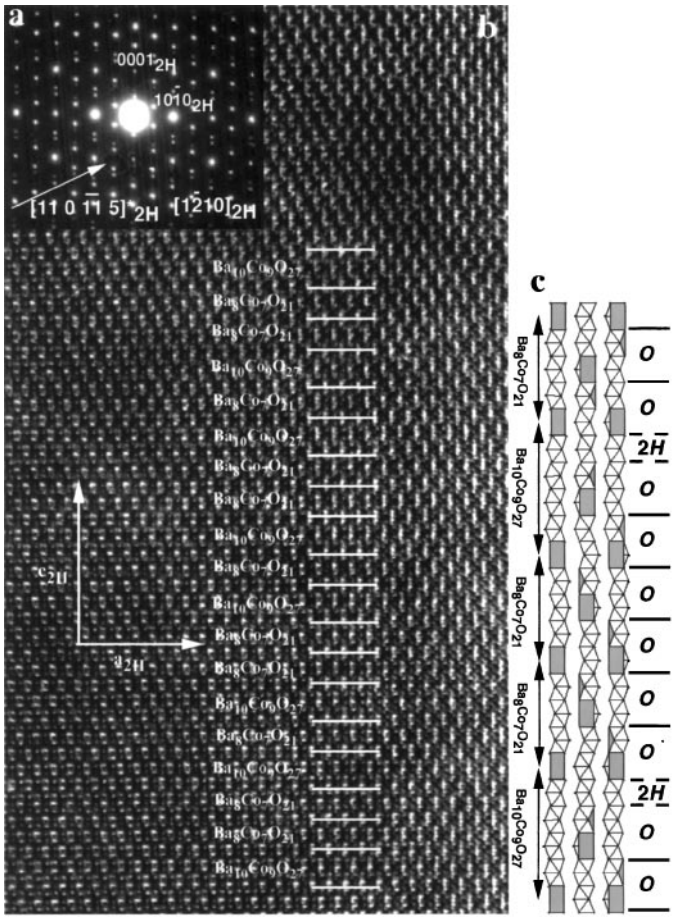

FIG. 6. (a) SAED and (b) HREM of $Ba_{44}Co_{39}O_{117}$ along $[1\bar{2}10]_{2H}$. (c) $Ba_{44}Co_{39}O_{117}$ structural model.

$5/44(2c^*_{2H})$. Therefore, $5(Ba_8Co_6O_{18})$ blocks and $6(Ba_8Co_8O_{24})$ blocks intergrow, per unit cell, along the *c*-axis. From the HREM image, the $\alpha = 5$, $\alpha = 6$ values are confirmed. An ordered intergrowth between $Ba_8Co_7O_{21}$ and $Ba_{10}Co_9O_{27}$ according to the sequence 2:1:1:1 is observed. Forty-four layers, 20 $Ba_8Co_2O_{18}$ and 22 Ba_8O_{24}, constitute the unit cell of the $Ba_{44}Co_{39}O_{117}$ phase, leading to a $[1TP{:}6O_h][1TP{:}6O_h][1TP{:}8O_h][1TP{:}6O_h][1TP{:}8O_h]$ polyhedra sequence in every row (Fig. 6c).

These three new phases are members of the $(Ba_8Co_6O_{18})_\alpha(Ba_8Co_8O_{24})_\beta$ orthorhombic polysomatic series and they can be described as ordered intergrowths of *o*-8:7 and *o*-10:9 phases. Between such phases, four terms of the series appear, which can be considered as recombination structures (18) of the above phases. Their unit cells are a consequence of the following intergrow paths:

$Ba_{26}Co_{23}O_{69}$: 2(*o*-8:7)/1(*o*-10:9)
$Ba_{44}Co_{39}O_{117}$: 2(*o*-8:7)/1(*o*-10:9)/1(*o*-8:7)/1(*o*-10:9)
$Ba_{18}Co_{16}O_{48}$: 1(*o*-8:7)/1(*o*-10:9)
$Ba_{28}Co_{25}O_{75}$: 1(*o*-8:7)/2(*o*-10:9).

As a consequence, the modulation vectors corresponding to these phases are directions between $m = 1/8$ and $m = 1/10$, i.e., those corresponding to *o*-8:7 and *o*-10:9. The upper term of the series is 2H-BaCoO3, but terms lower than that corresponding to *o*-8:7 have not been encountered. In fact, any term with a ratio $\alpha/\beta > 1$ should require that the orthorhombic $Ba_8Co_2O_{18}$ layers were not equivalent, thus reinforcing the idea that *o*-8:7 is the lowest term of this series.

According to the above reasoning, the new members reported in this paper must be regarded as the ordered intergrowth between structural slabs of one-half unit cell of the *o*-8:7 phase (called *O*) and one $Ba_8Co_8O_{24}$ 2H-block (referred as 2H) in different ratios. The new polysomatic structures, $Ba_{26}Co_{23}O_{69}$, $Ba_{28}Co_{25}O_{75}$, and $Ba_{44}Co_{39}O_{117}$ are formed by a mixture of such structural slabs in the following way: (*OO2HOOOO*), (*OO2HOO2HOO*), and (*OO2HOOOOOO2HOO*).

ACKNOWLEDGMENT

We acknowledge the financial support of CICYT (Spain) through Research Project MAT98-0648.

REFERENCES

1. J. B. Thompson, *Am. Mineral.* **63,** 239 (1978).
2. J. C. Grenier, J. Darriet, M. Pouchard, and P. Hagenmuller, *Mater. Res. Bull.* **11,** 1219 (1976).
3. J. C. Grenier, M. Pouchard, and P. Hagenmuller, *Struct. Bonding* **47,** 1 (1981).
4. H. D. Megaw, *Proc. Phys. Soc.* **58**(2), 133 (1946).
5. E. F. Bertaut, P. Blum, and A. Sagnieres, *Acta Crystallogr.* **12,** 149 (1959).
6. J. Darriet and M. A. Subramanian, *J. Mater. Chem.* **5**(4), 543 (1995).
7. P. D. Battle, G. R. Blake, J. Sloan, and J. F. Vente, *J. Solid State Chem.* **136,** 103 (1998).
8. M. Zakhour-Nakl, J. B. Claridge, J. Darriet, F. Weill, H. C. Zur Loye, and J. M. Pérez-Mato, *J. Am. Chem. Soc.* **122,** 1618 (2000).
9. J. Lander, *Acta Crystallogr.* **4,** 148 (1951).
10. J. J. Randall and L. Katz, *Acta Crystallogr.* **12,** 519 (1959).
11. K. Boulahya, M. Parras, and J. M. González-Calbet, *J. Solid State Chem.* **142,** 419 (1999).
12. K. Boulahya, M. Parras, and J. M. González-Calbet, *J. Solid State Chem.* **145,** 116 (1999).
13. K. Boulahya, M. Parras, and J. M. González-Calbet, *Chem. Mater.* **12**(1), 25 (2000).
14. K. Boulahya, M. Parras, J. M. González-Calbet, and A. Vegas, *J. Solid State Chem.* **151,** 77 (2000).
15. K. Boulahya, M. Parras, and J. M. González-Calbet, *Chem. Mater.* **12**(9), 2727 (2000).
16. D. R. Veblen, *Am. Mineral.* **76,** 801 (1991).
17. D. R. Veblen, *Mineral. Soc. Am. Rev. Mineral. A* **9,** 189 (1981).
18. J. Lima-de-Faria, E. Hellner, F. Liebau, E. Makovicky, and E. Parthè, *Acta Crystallogr. A* **46,** 1 (1990).